APPLICATION OF SOL GEL DERIVED PZT THIN FILMS TO THE DESIGN AND FABRICATION OF LAMB WAVE SENSING DEVICES

Yu, Jyh-Cheng[*§], Lin, Huang-Yao[*], and Tsai, Jong-Xin[*]

[*] Department of Mechanical and Automation Engineering
National Kaohsiung First University of Science and Technology
No. 2, Juoyue Rd., Nantz District, Kaohsiung 811, TAIWAN

[§] Center for Micro/Nano Science and Technology, National Cheng Kung University
No.1, Ta-Hsueh Road, Tainan 701, TAIWAN

Abstract: This study addresses the design and the fabrication of Lamb-wave sensing devices using sol-gel derived lead zirconate titanate (PZT) thin films, and illustrates the preliminary results for possible applications. The device adopts a two-port structure on the composite membrane of PZT and SiN_x. The response difference between the delay-line and resonator are compared. The design of the reflecting grating is derived using COM theory to produce a sharp resonant peak. The device is designed to excite the lowest mode of Lamb waves with a phase velocity less than the speed of sound in the contacting liquid to reduce energy dissipation, and thus suitable for liquid sensing applications. The mass and viscosity effects from the theoretical expression reveal the applications and the constraints of the device in liquid sensing. The fabrication issues of the proposed material structure are presented. Multiple layers of PZT films are coated using Sol-Gel technique because of the cost advantage and the high electromechanical coupling effect over other piezoelectric films. A thin film of $(La_xSr_{1-x})MnO_3$, LSMO, is introduced as a buffer layer between the PZT film and the electrodes to enhance the piezoelectric characteristics and the fatigue resistance. The vibrating membrane for the acoustic waves is anisotropicaly etched using KOH. This study investigates the possible applications in liquid density sensors and biosensors. Theoretical estimations of the mass and the viscosity effects are also compared with the experimental results. The resonant frequency has a good linear correlation with the density of low viscosity liquids, which demonstrate the feasibility of mass sensing. At last, a sensitized film is coated on the membrane cavity, and shows the potential of biosensing.

Keywords: FPW resonator, pressure sensor, biosensor, PZT, Sol-Gel

1. Introduction

The phase velocity and damping of acoustic wave devices are sensitive to external disturbances such as temperature, a differential pressure, additive mass, and the viscosity of loading liquid, which makes the device suitable for sensor applications[1][2]. The excitation and the detection of acoustic waves are most readily accomplished by the use of interdigital transducers (IDTs) [3] on piezoelectric substrate. Among them, the phase velocity of lamb waves, unlike the velocity of surface acoustic wave (SAW), depends on the thickness of the propagating plate. There are several advantages of Lamb wave sensors over SAW sensors in the applications of chemical sensing. A slow mode of propagation will reduce radiation loss when in contact with liquids. The access to the backside of the etched membrane also facilitates the isolation design of the transducer from loading liquid.

The design of IDT and the membrane thickness determines the wave length and the response characteristics. The lowest antisymmetric mode, A_0 of lamb waves, also called "flexural plate wave" (FPW), would be excited if the thickness of the propagating plate is less than 1/4 of the acoustic wavelength [4]. The detection of measurands can be identified by the phase shift or the deviation of resonant frequency. To increase the differentiability and the sensitivity of the resonant frequency shift, reflecting gratings are added to the FPW devices [5][6].

The membrane of FPW devices is often etched from a bulk piezoelectric substrate such as quartz (SiO_2), lithium tantalate ($LiTaO_3$), and lithium niobate ($LiNbO_3$). Piezoelectric thin films over silicon based membrane have the cost advantage over bulk materials, which has attracted a lot of research interests. Laurent *et al.*[7] addressed the configuration design of the FPW devices using AlN and ZnO on silicon membrane, and showed that the FPW device has a large mass sensitivity compared to other acoustic devices. Costello *et al.*[8] proposed a simple theory for the mass sensitivity of a delay-line oscillator with ZnO on silicon nitride membrane, and modeled the attenuation of plate waves in contact with viscous liquids. Weinberg *et al.*[9] derived the fluid-damping model for resonant FPW devices.

Acoustic wave devices can be applied to biosensing when the sensing area of a delay line is coated with a bio-sensitized film[10]. The interlock of antigen and antibody is detected by the additve mass effect of a FPW device. Pyun etc. [11] deposited an immunoaffinity layer on the membrane of the FPW device to detect Escherichia Coli (E. Coli). The gravimetric detection limit is less than 6 (ng) at a 32 (μm) thick sensitive layer in aqueous media.

The electromechanical coupling effect and the dielectric constant of PZT are much higher than AlN and ZnO. Also, sol-gel deposition is promising because of the cost advantage for commercial applications. However, the polycrystalline structure of PZT and the high-temperature in annealing process might incur cracking and diffusion of structure layers. The deposition of buffer layers, such as LSMO, between PZT thin film and structure layers can improve the piezoelectric characteristics, fatigue resistance, ferroelectricity, and reduce leaking current [12].

Though many literatures address possible applications of FPW devices, mass, stress, and viscosity effects might couple when the device is in contact with liquid, which affects sensing selectivity. Very few address the practical issues related to sensor fabrication and measurement that are important in liquid and biological sensing. This study will discuss the design and the fabrication for the FPW device using sol-gel derived PZT films on silicon nitride membrane. We will investigate some important fabrication issues such as the influence of material structure and process parameters. Constraints and solutions of the device in liquid and biological sensing will be presented. Finally, the experimental result is compared with the theoretical estimation.

2. Design of FPW Devices

The proposed FPW device adopts the structure of two-port IDT on a composte membrane consisted of piezoelectric layers, buffer layer, and silicon nitride supporting membrane. The schematic view of the device is shown in Figure 1. Two reflectors are added to the outsides of delay-line for a resonator. To excite the lowest mode of flexural plate wave, the thickness of the composite membrane is selected to be 5% or less of the acoustic wavelength λ.

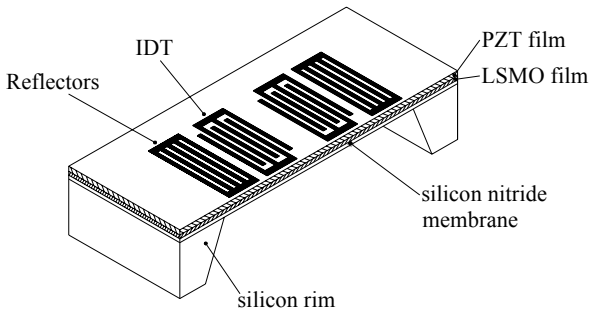

Figure 1. Schematic View of FPW resonators

2.1. Estimation of Phase Velocity

Consider the A_0 mode of FPW propagating on a thin plate; the phase velocity of the plate regime can be expressed by a simple asymptotic expression [13]:

$$v_P = \left(\frac{B}{M}\right)^{1/2} \tag{1}$$

where $B = \left(\frac{\lambda}{2\pi}\right)^2 \frac{E' d^3}{12}$ is the bending stiffness,

$E' = E/\left(1-\upsilon^2\right)$ is the effective Young's modulus,

E is the actual Young's modulus,

ν is Poisson's ratio,

d is the plate thickness, and

M is the mass per unit area of a homogeneous isotropic plate.

For the application of fluid and biosensing , the phase velocity of the acoustic wave has to be smaller than the velocity of sound in water to reduce the radiation energy loss. Other design parameters are determined from the tradeoff between the device size. The more pairs of IDT, the smaller insertion loss and the wider bandwidth. The increase of the overlap length of IDT will decrease the insertion loss and increase the transmission effect. The proposed device assumes 20 pairs of electrodes for both IDTs, the overlap length of IDT to be 50λ, and the separation between the IDTs to be 10λ.

The material structure of the proposed FPW device is assumed Pt (0.15μm) / Ti (0.02μm) / PZT (1μm) / LSMO (0.1μm) / SiN_x (1.2μm). Table 1 lists the mechanical properties of the material system [16]. The PZT properties are assumed from bulk material. The $(La_xSr_{1-x})MnO_3$, LSMO, is a buffer layer between PZT and SiN_x. The material properties of LSMO are not available and assumed to be the same as the PZT film. The mass effect of the Pt and the Ti are neglected.

Table 1 The material properties of the composite plate

	SiN_x	PZT / LSMO
Thickness (μm)	1.2	1 (PZT) + 0.1 (LSMO)
Young's modulus (E, N/m^2)	$3.85*10^{11}$	$8.6*10^{10}$
Poisson ratio (v)	0.27	0.25
Density (ρ, kg/m^3)	3100	7600
M (kg/m2)	0.00372	0.00836

The total thickness of the composite membrane is 2.3 (μm). The material parameters of the composite membrane as shown in Table 2 estimated from the composite plate theory. The estimated phase velocity is 235 (m/s) from Eq.(2), and the resonant frequency of the device in air is f_{air} = 5.88 (MHz) for the wavelength of 40 (μm).

Table 2 The parameters of the composite membrane

E	$2.42*10^{11}$ (N/m^2)
M	0.1176 (N/m^2)
ν	0.26
E'	$2.6*10^{11}$ (N/m^2)
B	6497.93 (N/m)

3. Sensing Mechanism of the FPW Device

3.1. Loading Effects of Contact Liquid

When the device is in contact with liquid, it will introduce additional stiffness effect due to liquid weight and additional mass effect due to the agitation of the liquid. The phase velocity of the plate regime subject to a tensile stress and liquid loading can be well approximated as follows [13]:

$$v_P = \left(\frac{T_x + B}{M + \rho_F \delta_E + M_\eta}\right)^{1/2} \tag{2}$$

where T_x is the component of in-plane tension in the x direction,

$\rho_F\delta_E$ is the mass effect,
δ_E is the evanescent decay length,
ρ_F is the density of the fluid, and
M_η is the viscosity effect.

The evanescent decay length is given in Eq.(3) and can be further simplified if the phase velocity is much less than the velocity of sound in the contact liquid.

$$\delta_E = \left(\frac{\lambda}{2\pi}\right)\left[\left(1-\frac{v_P}{v_F}\right)^2\right]^{-1/2} \approx \left(\frac{\lambda}{2\pi}\right) \quad (3)$$

The viscosity effect is the mutiply of the liquid density and the viscous decay length:

$$M_\eta = \frac{\rho_F\delta_V}{2} \quad (4)$$

Where $\delta_V = \left(\frac{2\eta}{\omega\rho_F}\right)^{1/2}$ is the viscous decay length,

ω is the operating angular frequency, and
η is the shear viscosity.

Loading liquid will introduce additive mass and tension effects to the membrane, and result in the deviation of phase velocity. The additive mass is due to the agitation of loading liquid and is a function of liquid density and viscosity. Liquid pressure will result in tensile stress distributed in the membrane. The density sensitivity and tension sensitivity of the perturbation of phase velocity are as follows:

$$\frac{\Delta v_p}{v_p} = \frac{\Delta f_{A_0}}{f_{A_0}} = s_m \times (\delta_E \Delta\rho_F) + s_T \times \Delta T_x \quad (5)$$

where $s_m = -\frac{1}{2(M+\rho_F\delta_E)}$ and $s_T = \frac{1}{2(T_x+B)}$

From Eq.(5) we can see that the device could be a transducer for liquid density and membrance stress. If the mass effect due to liquid density is small compared with the unit membrance mass, the deviation coefficient of the A_0 resonant frequency will be in linear proportional to the liquid density for low viscosity liquids. Eq.(2) shows that liquid viscosity will introduce additional viscosity effeect to the mass term. However, we can't differentiate the velocity perturbations between liquid density (ρ_F) and shear viscosity (η) because the density and viscosity are coupled in the viscosity effect as shown in Eq.(4). In another word, the proposed device is not suitable for the density sensing of viscous liquids solely via the resonant frequency deviation.

Also, if the in-plane tension is small compared with the membrance stiffness, deviation coefficient of the A_0 resonant frequency will be in linear proportional to the in-plane stress of the membrane. Since the tensile stress is in proportional to the differential pressure, the FPW device is suitable for a liquid pressure sensor as well.

3.2. Density Sensing of Low Viscosity Liquids

The viscosity effect in Eq.(2) for a low viscosity liquid is negligible and the phase velocity will be influenced solely by the mass effect ($\rho_F\delta_E$) that is determined by the evanescent decay length. However, if the loading liquid is a small droplet on the thin plate and the contacting surface is not hydrophilic, the droplet will not spread out evenly and remain hemispherical as shown in Figure 2. Since only the evanescent decay length of the loading droplet will contribute the mass loading effect and the shape of the droplet can't be accurately controlled, the change of the phase velocity usually is not in proportional to the number of liquid droplets. Therefore, the liquid is suggested to fill up the cavity if the device is used to detect the mass effect. The liquid density will determine the low viscosity liquid loading as long as the filled liquid level is higher than the evanescent decay length as shown in Figure 3.

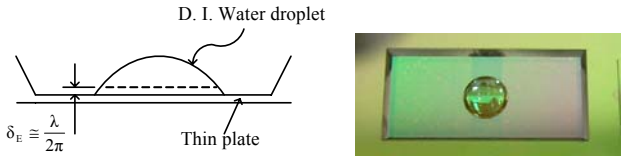

Figure 2 The liquid droplet on the FPW device

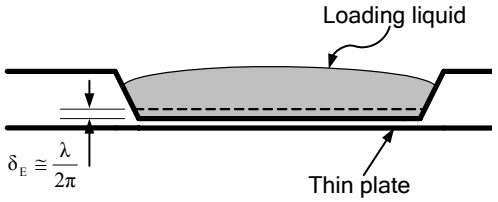

Figure 3 The evanescent decay length for the liquid loading of a FPW device

The calculated phase velocity for the composite membrane in air is about 235 ($m{\cdot}s^{-1}$) which is much smaller than the speed of sound in water, 1482 ($m{\cdot}s^{-1}$). The stiffness of the membrane is estimated using the composite plate theory. The calculated sensitivities in our case are s_m =-2.78(m^2/N)=-278(cm^2/g) and s_T =7.69*10^{-5}(m/N). Assuming 5 (mg) of water is loaded on the cavity, the average tensile stress along the wave propagating direction can be estimated from a finite element analysis. The estimated frequency deviation due to the mass loading of water is about -0.94 (MHz) and the frequency deviation due to the tensile effect is only +1.24 (Khz). The tension effect due to the liquid pressure can be ignored when compared with the mass loading effect.

When the device cavity is filled up with different liquids, the resonant frequency deviation will relate to the liquid density, and thus can be used as a density sensor. We can estimate the phase velocity for the device loaded with three low viscosity liquids as shown in Table 3.

Table 3 Estimated resonant frequency of the FPW device loaded with low viscosity liquids

	IPA	Water	Saline solution
Density (Kg/m^3)	787	1000	1200
Viscosity N-s/m^2	0.0025	0.001	~0.0015
Phase Velocity (m/s)	197.48	190.05	183.77
Resonant Frequency (MHz)	4.94	4.75	4.59

3.3. Biosensing Applications

The device can be applied to a biosensor that may detect the absorption or attachment of a layer of particular

molecules on the sensing region. The phase velocity of the device can be expressed as below:

$$v_P \cong \left(\frac{B}{M + \rho_F \delta_E + M_\eta + m_{sorptive} + \Delta m} \right)^{1/2} \quad (6)$$

where $m_{sorptive}$ is the mass per unit area of any selective biological or chemically sorptive layer, and Δm is the detectable added mass per unit area. In this study, $m_{sorptive}$ and Δm can be considered as the antibody layer and the locked-in antigen. The sensitivity to the detectable added mass will be as follows:

$$\frac{\Delta v_p}{v_p} = -\frac{1}{2\left(M + \rho_F \delta_E + M_\eta + m_{sorptive}\right)} \times (\Delta m) \quad (7)$$

To detect the frequency deviation due to the interlock of antigen and antibody, the proposed sensor design consists of two Lamb wave devices as illustrated in Figure 4. The first one is applied to detect external perturbation and the other one is filled with the reference solution. When the heights of both liquids exceed the evanescent decay length, the mass loading and viscosity will be the same. Here, the comparison of the two devices can isolate the added mass due to antigen bonding and compensates unnecessary perturbation.

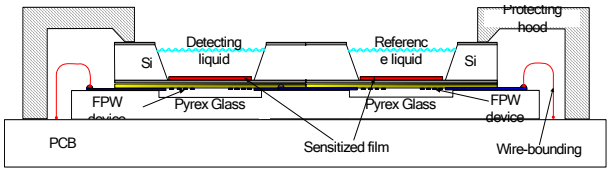

Figure 4 Schematic diagram of biosensing applications

We then find that the minimum detectable added mass, $\Delta m_{\min}$, in this fluid-loaded case with a sorptive film is just

$$\Delta m_{\min} = \frac{1}{s_m} \left(\frac{\Delta f_{\min}}{f} \right) \quad (8)$$

where $\Delta f_{\min}$ is the minimum significant frequency shift. Assume the viscosity effect and the weight of the selective biological sorptive layer are negligible. The estimated sensitivity of the device is –278 (cm^2/g). If the minimum differentiable frequency shift is 100 (Hz), the minimum mass change, $\Delta m_{\min}$ could be detected and examined is approximately $7.6*10^{-8}$ (g/cm^2). Equation (7) shows that the mass loading part $\rho_F \delta_E$ has a great influence on the sensitivity, where $\delta_E = \lambda/2\pi$. For thinner membranne and smaller design of wavelength, the higher the sensitivity.

4. Design of Reflecting Grating

The design of the reflecting grating of a FPW resonator can be derived from a two-port SAW resonator over a bulk PZT modeled using the COM theory[15]. There are three basic elements in the modeling of a typical SAW resonator: IDT, spacing, and reflector that can be described by three complex transmission matrices of [T], [D], and [G] respectively as shown in Figure 5. Matrix [T] is a 3×3 transmission matrix for the IDTs, including both the acoustic and the electric parameters. The terms, *a* and *b,* represent the incident and the reflected electrical signals respectively. Matrix [D] is a 2×2 matrix for the acoustic transmission line between IDTs and gratings. Matrix [G] is a 2×2 matrix for the SAW reflection grating to describe the relationship between the acoustic transmission and reflection responses W_i.

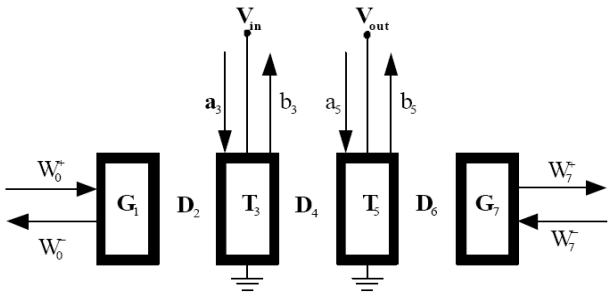

Figure 5 Representation of two-port resonator building blocks

Assume absorbers are applied to the outside of both reflection gratings; there will be no incident acoustic wave for the gratings G_1 and G_7. Often there is no input electrical signal for the output IDT. Considering all the boundary conditions above, we can obtain the estimationof the transmission coefficient S_{21}.

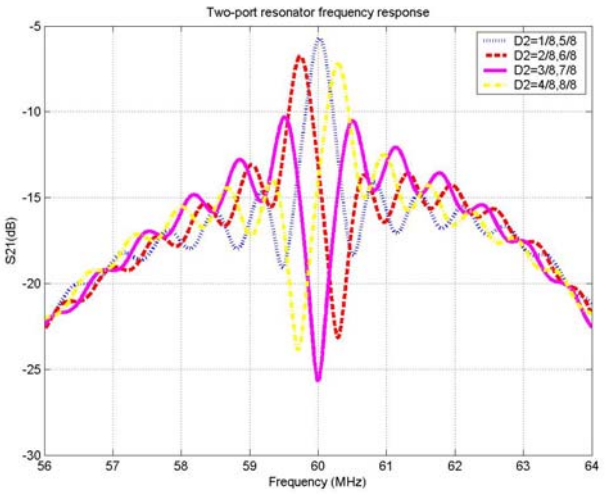

Figure 6 Two-port SAW resonator frequency response

The simulation parameters used here are as follows: acoustic wavelength is 40 (μm) with uniform finger spacing, and the phase velocity of bulk PZT is 2400 (m/s). The reflection phase, θ, is determined by the position of standing wave at the reference plane relating the sign of reflected-to-incident surface waves entering the reflection grating, which will affect the spacing design between the gratings and adjacent IDTs (D_2 and D_6). The determination of reflecting phase is difficult and often depends on the experimental for the material combination of the piezoelectric substrate and the reflecting electrodes [15]. The reflection coefficient for the PZT thin film and Pt/Ti reflecting grate is not available. However, since PZT is a strong piezoelectric, like lithium niobate, the reference phase $\theta = 0^\circ$ is assumed for the open circuit design of reflector. The number of reflection grating is set 40 to form standing waves to reduce insertion loss. As

shown in Figure 6, the spacing between the gratings and adjacent IDTs will affect the resonant pattern, and (*D2*) is designed to be (1/8+n/2)λ to produce a sharp resonant peak. The derived reflector design will be applied to the FPW device to increase the differentiablity of frequency deviation due to liquid loading.

5. Device Fabrication

5.1. Fabrication Procedure

The fabricating procedure of the FPW resonator includes the coating of piezoelecric layer, the silicon etching, and the lift-off of IDT as shown in Figure 7. The materials system of the resonator is assumed Pt/Ti/PZT/LSMO/SiN_x. The LSMO and the PZT thin films are multiple-coated by sol-gel techniques. The electrodes of the IDT are deposited using E-beam PVD and patterned for the period of 40 (μm) using lift-off. The back cavity is then patterned on SiN_x using RIE. Finally, the membrane cavity of the device is fabricated using KOH anisotropic etching (30ºC, 80%). The final composite membrane is consisted of 1.2 (μm) silicon nitride and 1.1 (μm) PZT layer. The size of the rectangular membrane is about 4.2×2.7(mm).

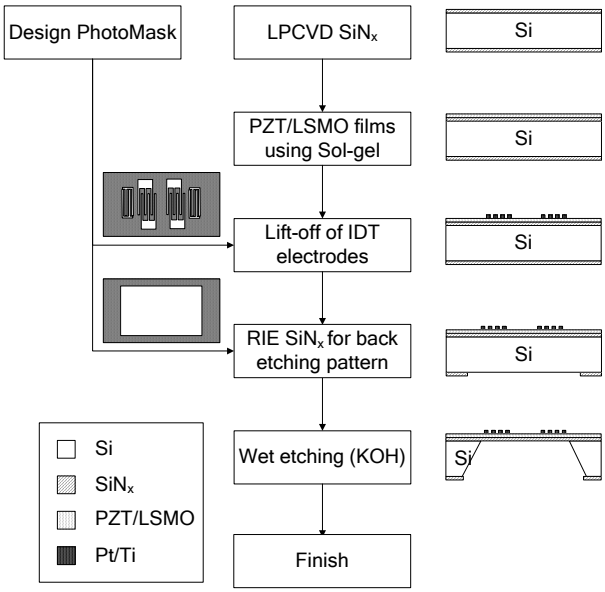

Figure 7 Fabrication procedure of the FPW device

5.2. Sol-Gel Deposition of PZT

The sol-gel PZT thin films require heat treatment to transform into polycrystalline piezoelectric layer. Furnace heating is used in this study. Higher heat treatment temperature might improve the material characteristics of PZT, however severe thermal stresses may crack the film due to incompatibility among constituent layers of the composite membrane. The PZT thin films are annealed at 650°C in the oven to transform the solution gel into polycrystalline structure. The comparison of the XRD results in Figure 8 shows that the LSMO buffer layer improves the perovskite structure without the Pyrochlore phase at a relatively low annealing temperature.

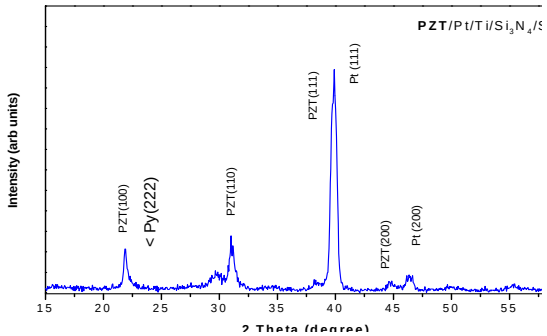

(a) PZT(4L)/Ti/Pt/SiN_x/Si

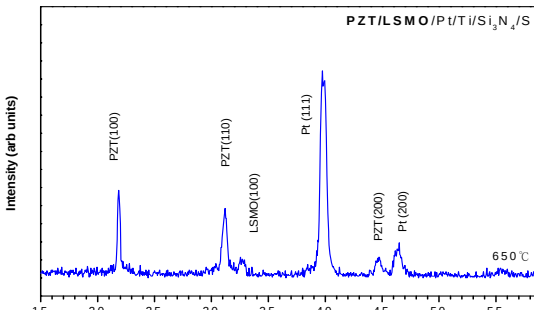

(b) PZT(4L)/LSMO(2L)Ti/Pt/SiN_x/Si

Figure 8 XRD of the PZT films

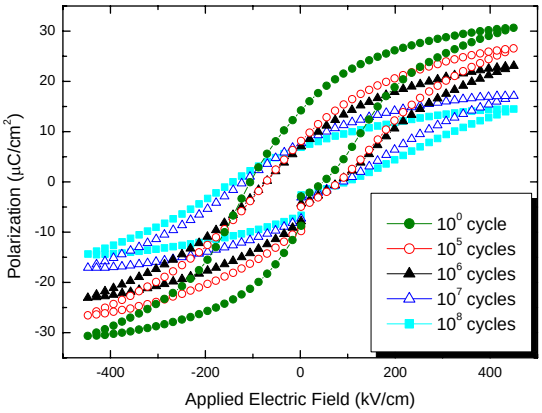

Figure 9 The fatigue characteristics for the PZT film without LSMO buffer layer

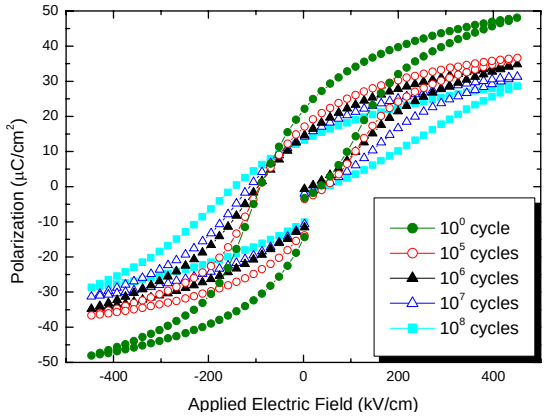

Figure 10 The fatigue characteristics for the PZT film with LSMO buffer layer

The LSMO buffer layer between PZT and SiN_x also enhances the piezoelectric characteristic and prevent possible cracking of PZT. As seen from the comparison between Figure 9 and Figure 10, the LSMO buffer layer not only enhances the Residual Polarization but also decrease the polarization decay due to fatigue loading that is very important for resonant devices.

5.3. Deposition of the Bio-Sensitized Film

The bio-sensitized film is deposited on the cavity side of the membrane. The first step is to deposit A Au/Ti adhesion layer is used between the antibody layer and the SiN membrane. The depositing result is examined using immuofluorescence as illustrated in Figure 11. The luminous points shows that the antibody layer is successfully coated on the membrane area.

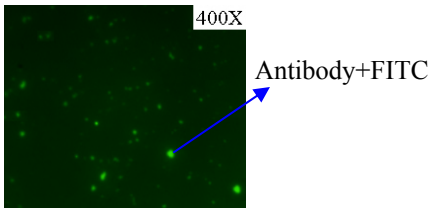

Figure 11 Coating of bio-sensitized films

6. Experimental Results And Discussions

6.1. The Signals of FPW Delay Line and Resonator

The frequency responses of the FPW delay line and the FPW resonator are measured using a network analyzer (HP8753 ES). The frequency responses of the FPW delay line and the FPW resonator are shown in Figure 12. The measured resonant frequency without liquid loading is 5.53 (MHz) that is pretty close to the theoretical estimation of 5.88(MHz). The difference might be due to the use of the bulk material properties in the theoretical estimation because the PZT film properties are not available. The resonator has a more obvious resonant signal than the delay line design, although sharp peak is not observed, which might be due to the polycrystalline structure of PZT.

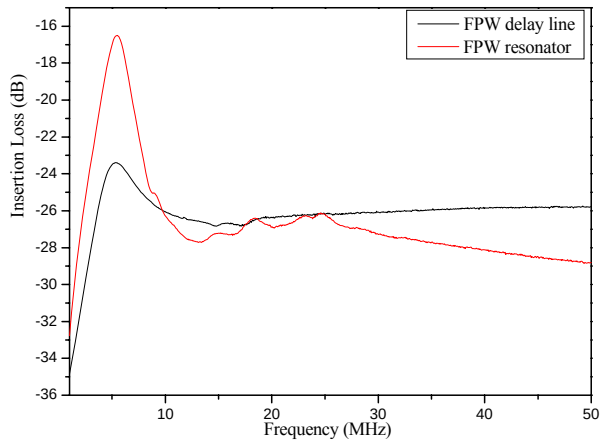

Figure 12 The S_{21} frequency response of the FPW devices

6.2. Gravimetric Sensing Using the FPW Resonator

Three low viscosity liquids, DI Water (1 g/cm^3), IPA (0.787 g/cm^3) and saline solution (1.2 g/cm^3), are applied to the resonator to simulate the variation of additive mass to the membrane. The viscosity effect is negligible compared with the mass effect. The sensitivity analysis between the resonant frequency and the densities of the liquids is summarized in Figure 13. The theoretical relative density sensitivity for low viscosity liquids is -0.848 (Mhz/g·cm^{-3}), and the experimental sensitivity is -0.602 (Mhz/g·cm^{-3}). The results show that the resonant frequency and the liquid density have a good linear correlation despite a sensitivity difference., which demonstrates the feasibility of density sensing. The difference may be due to the use of the bulk material properties in the theoretical estimation because the PZT film properties are not available.

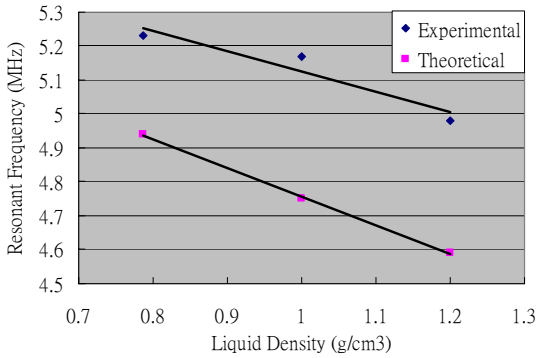

Figure 13 The sensitivity analysis between the resonant frequency and the density for low viscosity liquids

However, the phase velocity of FPW will be influenced by fluid density and shear viscosity of the high viscosity liquid from the theoretical analysis. We can't differentiate the velocity perturbations between liquid density and viscosity because the density and viscosity are coupled in the viscous effect. In another word, the liquid viscosity can't be determined by the frequency shift. Here, we compare two liquids, glycerol with viscosity of 934×10^{-3} (N-s/m^2) and a low viscosity saline solution with the same density (1.2 g/cm^3) to study the viscosity effect. From Table 4, we observe that the glycerol loading will introduce additional frequency deviation compared with the saline solution with the same density. Also, the viscosity effect of glycerol will cause more damping effect than the saline solution and increases the insertion loss.

Table 4 The viscosity effect on the resonant frequency and insertion loss

	Theoretical	Experimental	
	Frequency (MHz)	Frequency (MHz)	Insertion Loss (dB)
Saline solution	4.59	4.98	-33.38
Glycerol	4.49	4.73	-37.04

The experimental results also show the feasibility of biosensing applications. If the device is used in a

biosensing after the deposition of biosensitized film, the gravimetric sensitivity is about 10^3 (MHz/g cm^2).

7. Conclusions

This study has successfully fabricated the FPW resonator on the PZT piezoelectric thin films and compared with the modeling analysis. The fabrication process is presented and the influence of the process parameter is studied. The addition of the LSMO buffer layer improves the surface interface and the sensor reliability. Although the polycrystalline structure of PZT may obscure the resonant peak of the frequency response, it is good enough to differentiate the frequency deviation. The device is applied to the loading of various liquids. We have observed that the liquid loading will increase the insertion loss and decrease the resonant frequency that is consistent with theoretical prediction. The linear correlation between the resonant frequency and the density of low viscosity liquid demonstrates the feasibility of density sensing. Additional frequency deviation and insertion loss are observed for high viscosity liquids, which also matches fairly with the theoretical estimation. We have also successfully coated the sensitized layer on the membrane, and estimated the gravimetric sensitivity. The preliminary measurement result demonstrates the application feasibility of the Lamb wave device.

8. References

[1]. Vellekoop, M. J.,"Acoustic wave sensors and their technology", *Ultrasonic*, 36, 1998: 7-14.

[2]. Choujaa, A., Tirole, N., Bonjour, C., Martin, G., Hauden, D., Blind, P., Cachard, A., and Pommier, C., "AlN/silicon lamb wave microsensors for pressure and gravimetric measurements", *Sensors and Actuators* A, 46, 1995: 179-182.

[3]. White, R. M. and Voltmer, F. M. "Direct piezoelectric coupling to surface elastic waves", *Appl. Phys. Lett*., 7, 1965: 314-316.

[4]. Toda, K., "Lamb-wave delay lines with Interdigital electrodes", *Japanese Journal of Applied Physics*, 44, 1973: 56-62.

[5]. Joshi, S. G. and Zaitsev, B. D., "Reflection of ultrasonic Lamb waves propagating in thin piezoelectric plates", *Ultrasonics Symposium*, 1998: 423-426.

[6]. Nakagwa, Y., Momose, M. and Kakio, S., "Characteristics of reflection of resonators using Lamb wave on AT-cut quartz", *Japanese Journal of Applied Physics*, 43, 2004: 3020-3023.

[7]. Laurent, T., Bastien, F. O., Pommier, C., Cachard, A., Remiens, D., and Cattan, E., "Lamb wave and plate mode in ZnO/silicon and AlN/silicon membrane Application to sensors able to operate in contact with liquid", *Sensors and Actuators*, 2000: 26-37

[8]. Costello, B. J., Martin, B. A., and White, R. M. "Ultrasonic plate waves for biochemical measurements", *Ultrasonics Symposium*, 1989: 977-981

[9]. Weinberg, M. S., Dubé, C. E., Petrovich, A., and Zapata, A. M., "Fluid damping in resonant flexural plate wave device", *Journal of Microelectromechanical Systems*, 12(5), 2003: 567-576.

[10]. White, R. M., "Acoustic sensors for physical, chemical and biochemical applications", *IEEE Frequency Control Symposium*, 1998: 587-594

[11]. Pyun, J.C., Beutel, H., Meyer, J.-U., and Ruf, H.H. "Development of a biosensor for E. coli based on a flexural plate wave (FPW) transducer", *Biosensors & Bioelectronics*, 13(7-8), 1998: 839-845

[12]. Pan, H.-C., Chou, C.-C. and Tsai, H.-L., "Low-temperature Processing of Sol-Gel derived La0.5Sr0.5MnO3 Buffer Electrode and Integration with $PbZr_{0.52}Ti_{0.48}O_3$ Films Using CO_2 Laser Annealing" *Appl. Phy. Lett*. 83(15), 2003: 3156-3158.

[13]. White, R. M. et al., *Acoustic Wave Sensors Theory, Design, and Physico-Chemical Applications*, Academic Press, 1996.

[14]. Matsui, Y., Okuyama, M., Fujita, N., and Hamakawa, Y., "Laser annealing to produce ferroelectric-phase $PbTiO_3$ thin films", *J. Appl. Phys.* 52(8), 1981: 5107-5111

[15]. Campbell, C. K., *Surface acoustic wave devices for mobile and wireless Communications*, San Diego: Academic Press, 1998.

[16]. http://www.piezo-kinetics.com/PKI_700.htm

Contact info:

Yu, Jyh-Cheng （余志成）
Associate Professor
Department of Mechanical and Automation Engineering
National Kaohsiung First University of Science and Technology
No. 2, Juoyue Rd., Nantz, Kaohsiung 811, TAIWAN
Phone: +886-7-6011000 ext.2228 Fax: +886-7-6011066
Email: jcyu@ccms.nkfust.edu.tw
Website: www2.nkfust.edu.tw/~jcyu/